REVISTA INTERDISCIPLINAR DE PESQUISA EM ENGENHARIA

CILAMCE 2016
XXXVII IBERIAN LATIN AMERICAN CONGRESS ON COMPUTATIONAL METHODS IN ENGINEERING
BRASÍLIA - DF - BRAZIL

COMPUTATIONAL STUDY OF METHODS FOR FLUID STRUCTURE INTERACTION

Denner Miranda Borges

João Marcelo Vedovoto

João Rodrigo Andrade

dennermiranda@ufu.br

jmvedovoto@mecanica.ufu.br

jandrade@mec.ufu.br

MFLab - Laboratory of Fluid Mechanics, School of Mechanical Engineering, Federal University of Uberlandia

Av. João Naves de Ávila, 2121, Uberlândia, MG, 38408-196, Brazil

Aldemir Ap Cavalini Jr

aacjunior@mecanica.ufu.br

LMEst - Laboratory of Mechanics and Structures, School of Mechanical Engineering, Federal University of Uberlandia

Av. João Naves de Ávila, 2121, Uberlândia, MG, 38408-196, Brazil

Abstract. *This work presents the numerical simulations of problems of solid and fluid mechanics aiming a future fluid structure interaction, considering an immersed flexible beam. In recent years, a number of applications dedicated to flow-induced vibrations have been proposed in order to satisfy the increasing demand for high performance and safe operation of mechanical systems. The vibration response of aircraft wings, bridges, buildings, and engine blades, are frequently obtained by using fluid-structure interaction approaches. Therefore, the flow-induced vibrations are determined from the mathematical models of both the fluid and the submerged structure. A cantilever beam is used to demonstrate the efficiency*

of the proposed methods for the integrated solution of these domains. A finite element model based on the Euler-Bernoulli theory is used to obtain the dynamic responses of the beam. The fluid domain is simulated by using the equations of Navier-Stokes associated with the local ghost-cell immersed boundary method. The results show the method efficiency in dealing with corners and sharp geometries, as beams and airfoils, for fluid-structure problems considering immersed boundaries. Further research efforts will be dedicated to numerical tests for evaluate coupling algorithms, given the methodologies applied.

Keywords: *Fluid-structure interaction, Finite element model, Ghost-cell immersed boundary method, Flexible beams.*

1 INTRODUCTION

The fluid-structure interaction (FSI) commonly refers to the interaction between a fluid and a solid body, where the yield motions of the fluid and the solid are dependent on each other. Physically, this phenomenon can be interpreted as action and reaction efforts between the structure and the surrounding fluid flow. Therefore, the mathematical models used to solve this problem should take into account equations devoted to the motion of the fluid and the deformation of the structure.

Typically, this phenomenon involves a coupled interface that should be solved simultaneously. However, the requirement of the computational time is high, making the analysis for complex problems impractical. The solution of the coupled system may be accomplished by solving the two systems separately with the interaction effects determined by a coupled solution (Mitra *et al.*, 2008).

In this context, this contribution is devoted to evaluate different methodologies for the solution of both structural and fluid domain, considering a submerged cantilever beam. The dynamic response of beam is given by a finite element model formulated from the classic Euler-Bernoulli beam theory.

The methodologies for fluid domain commonly involves a body-fitted grids. Despite the known advantages of this method, a high computational effort is required for motion bodies. In FSI problems, where the time deformation of flexible structures as airplane wings, risers, and bridges are substantial, the analysis can be impractical. An alternative approach for the conventional body-fitted grids, is the use of cartesian meshes applying the immersed boundary method. Complex geometries and moving bodies can be simulated by using this methodology, once the mesh of the fluid and the body are treated separately. Although these advantages, a common problem in the immersed boundary methods is the difficult in leading with flows over corners and sharp geometries, as beams and airfoils (Andrade, 2015).

In the present work, a variation of the immersed boundary methods is used. The local ghost-cell immersed boundary (Berthelsen and Faltinsen, 2008) is a robust method which allows solving the problem of thin geometries, without loss of accuracy in the solution. The central difference scheme (CDS) is applied to express both the diffusive and advection contributions of the transport equations on a staggered grid. The results show the efficiency of this methodology to simulate immersed bodies and problems involving fluid-structure interaction.

2 MATHEMATICAL AND NUMERICAL MODELING

2.1 Structural domain

In this case, the finite element method is used to obtain the dynamic responses of a cantilever beam. The beam element is formulated from the classic Euler-Bernoulli theory. The main interest is the bending motion of the system, considering a homogeneous, elastic, and isotropic beam. Using the elementary beam theory, the 2-D beam or flexure element is developed. It consists of two nodal points and the nodal variables are the transverse displacements and the rotations.

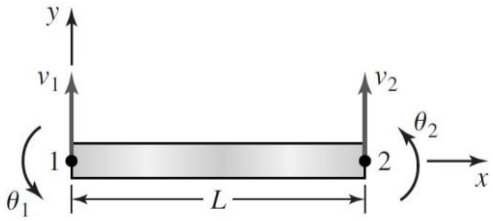

Figure 1. Nodal displacements of the beam element

The mass per unit length of the structure element is $m_i = \rho A$, where ρ and A are respectively the mass density and the cross sectional area of the beam element. The structural displacements of an element are approximated by using their nodal values given by:

$$\tilde{v}(x,t) = [N(x)]\{d(t)\} \tag{1}$$

Where $\{d(t)\}$ is the vector of time dependent nodal displacements and $[N(x)]$ is the matrix of shape functions, which indicates that the displacement and rotation fields of the beam element are expressed as linear combinations of displacements and rotations of the nodes. The mass matrix for the beam element is given by:

$$\left[m_{(e)}\right] = m_i \int_0^L [N(x)]^T [N(x)] dx \tag{2}$$

Assuming a linear elastic material, from the potential energy, the stiffness matrix can be obtained by:

$$\left[k_{(e)}\right] = \int_0^L E\,I \left[\frac{d^2[N(x)]}{dx^2}\right]^T \left[\frac{d^2[N(x)]}{dx^2}\right] dx \tag{3}$$

Therefore, the stiffness and elemental mass matrices ($k_{(e)}$ and $m_{(e)}$) are given by:

$$\left[m_{(e)}\right] = \frac{m_i L}{420}\begin{bmatrix} 156 & 22L & 54 & -13L \\ 22L & 4L^2 & 13L & -3L^2 \\ 54 & 13L & 156 & -22L \\ -13L & -3L^2 & -22L & 4L^2 \end{bmatrix} \tag{4}$$

$$\left[k_{(e)}\right] = \frac{EI}{L^3}\begin{bmatrix} 12 & 6L & -12 & 6L \\ 6L & 4L^2 & -6L & 2L^2 \\ -12 & -6L & 12 & -6L \\ 6L & 2L^2 & -6L & 4L^2 \end{bmatrix} \tag{5}$$

The differential equations that describes the dynamic behavior of the beam can now be written as follows:

$$\left[M_{(g)}\right]\left\{\ddot{d}\right\} + \left[C_{(g)}\right]\left\{\dot{d}\right\} + \left[K_{(g)}\right]\{d\} = F_{ext} \tag{6}$$

where $M_{(g)}$ and $K_{(g)}$ are the global mass and stiffness matrices (finite element model), respectively. In this case, the boolean matrix $[T_i]$ is used to determine the global model from the elementary finite element matrices as follow:

$$\left[M_{(g)}\right] = \sum_{i=1}^{n^\circ \text{ of elements}} \left[T_i\right]^T \left[m_{(e)}\right]\left[T_i\right] \tag{7}$$

$$\left[K_{(g)}\right] = \sum_{i=1}^{n^\circ \text{ of } elements} \left[T_i\right]^T \left[k_{(e)}\right]\left[T_i\right] \tag{8}$$

The matrix $C_{(g)}$ is the proportional damping matrix, given by:

$$\left[C_{(g)}\right] = \alpha\left[M_{(g)}\right] + \beta\left[K_{(g)}\right] \tag{9}$$

where α and β are the proportional damping coefficients. All externally applied forces in the beam are included in the term F_{ext}.

2.2 Fluid domain

The Navier-Stokes equations associated with the local ghost-cell immersed boundary method (LGC) is used to solve the fluid domain. The immersed boundary methods consist in represents an immersed body as a field of forces, inserted in the moving equations of fluid. The LGC method applied in this work consist in a special group of immersed boundary methods with direct boundary condition imposition.

A rectangular domain was used for the present simulations and it was discretized with a eulerian gridin a non-uniform cartesian frame. The governing equations for a viscous incompressible flow can be written as Eq. 10.

$$\frac{\partial(\rho u_i)}{\partial t} + \frac{\partial(u_i u_j)}{\partial x_j} = -\frac{\partial p}{\partial x_i} + \frac{\partial}{\partial x_j}\left[\mu\left(\frac{\partial u_i}{\partial x_j} + \frac{\partial u_j}{\partial x_i}\right)\right] + \vec{f}_i \tag{10}$$

In the Eq. (10), p is the pressure, ρ is the density of fluid, u_i and u_j are the components i and j of the vector velocity. The term $\vec{f}_i$ is the eulerian body force, and gives to the flow the presence of a solid body, respecting the conditions of contact fluid-solid.

The LGC consists in the use of local ghost cells obtained by unidimensional extrapolation performed in the direction of discretization term. These extrapolations are use to the calculus of derivatives in the cells near immersed boundary, where there is not a complete group of neighboring cells used in the discretization of the terms of Navier-Stokes equation.

To identify the immersed boundary influence, it is provided three kinds of grid cells which give rise to boundaries immersed inside the computational domain. The first step of the method is to establish the grid-interface relation with a given immersed boundary description, such as parametrized curve/surface or triangulation. In this step, based on Berthelsen and Faltinsen (2008), all Cartesian grid center nodes are split into the following categories:

1. Solid-cells: as the name suggests, are cells whose nodes lie inside the solid body in solid phase.

2. Neighboring-cells: grid points in the fluid phase with one or more, depending on discretization order method, neighboring points in the solid phase.

3. Fluid-cells: cells whose nodes lie outside the body, in the fluid phase and far from the immersed boundary.

4. Forcing-cells (for velocity points): grid velocity points in the fluid phase with one solid-cell pressure point as neighbor such that the pressure equation can not be applied. These points have its velocities values imposed by interpolation strategy and are not included on the velocity matrix system.

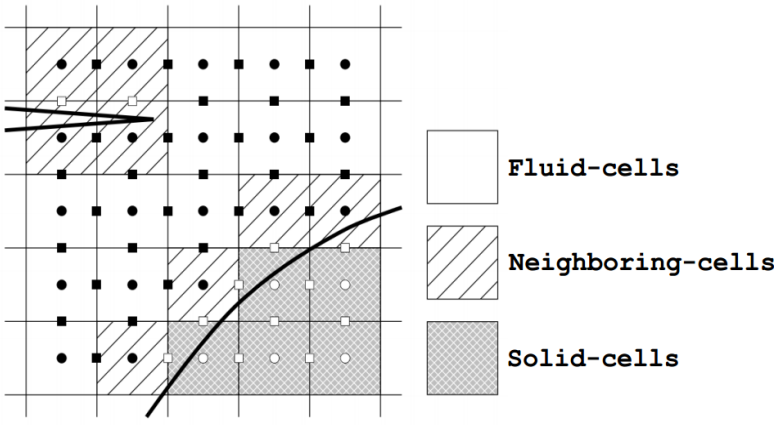

Figure 2. Classification of fluid cells, reprinted from Berthensen and Faltinsen (2008). Active points of pressure (●); inactive points of pressure (○), active points of velocity (■) and inactive points of velocity (□).

The Navier-Stokes equations are solved only for active cells. The inactive points of velocity out of boundary are imposed by unidimensional interpolation function, considering neighbor active points. By this way, the velocity of a boundary point $x_{i+1/2,\,j}$ is given by a third degree interpolation function:

$$u_{i+1/2} = \sum_{s=i-2}^{j} \left(\prod_{t=i-2, t\neq s}^{j} \frac{x_{i+1/2} - x_{t-1/2}}{x_{s-1/2} - x_{t-1/2}} \right) \frac{x_{i+1/2} - x_{\Gamma}}{x_{s-1/2} - x_{\Gamma}} u_{s-1/2} + \prod_{t=i-2}^{j} \frac{x_{i+1/2} - x_{t-1/2}}{x_{\Gamma} - x_{t-1/2}} u_{\Gamma} \tag{11}$$

where u_{Γ} is the velocity in the solid wall of position x_{Γ}, and $\{u_{i-1/2}, u_{i-3/2}, u_{i-5/2}\}$ are subsequent values of velocity of neighbor points $\{x_{i-1/2}, x_{i-3/2}, x_{i-5/2}\}$. The subindex j is omitted for simplification. If a point can be interpolated over a direction, the velocity of this point can be obtained by a pondered function of each direction, given by:

$$u_{i+1/2,\,j} = \gamma_x u^{x}{}_{i+1/2,\,j} + \gamma_y u^{y}{}_{i+1/2,\,j} \tag{12}$$

Where γ_x and γ_y are the pondered coefficients:

$$\gamma_x = \left[1 + \left(\frac{a\Delta x}{b\Delta y} \right)^2 \right]^{-1} \tag{13}$$

$$\gamma_y = \left[1 + \left(\frac{b\Delta y}{a\Delta x} \right)^2 \right]^{-1} \tag{14}$$

and $a\Delta x$ and $b\Delta y$ are the distances between immersed boundary and boundary point in directions x and y respectively.

The discretization of derivative terms is obtained by scheme of centered differences, using a group of active velocity points. In case of insufficient active points for the calculus of derivative term, as example points inside the immersed boundary, showed in Fig. 3, a numerical approach is performed to obtain the derivatives terms.

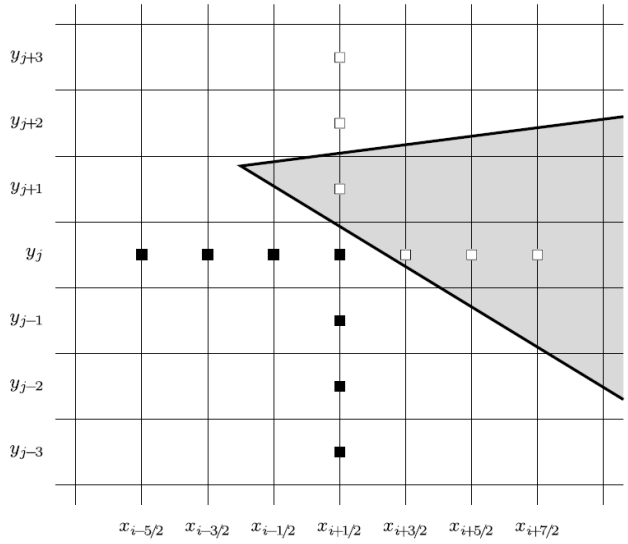

Figure 3. Irregular points inside the immersed boundary, in direction x. Reprinted from Berthensen and Faltinsen (2008).

In Fig. 3, a group of neighbor faces is used to calculate the derivatives in directions *x* and *y*, given by:

$$\mathbb{D}_{xy} = \left\{ u_{i-1/2,j}, u_{i+1/2,j}, u^{g}_{i+3/2,j}, u^{g}_{i+1/2,j+1}, u_{i+1/2,j-1}, v^{g}_{i,j+1/2}, v_{i-1,j+1/2}, v_{i,j-1/2}, v_{i-1,j-1/2} \right\} \tag{15}$$

where $u^{g}_{i+3/2,j}$, $u^{g}_{i+1/2,j+1}$, and $v^{g}_{i,j+1/2}$ are the ghost velocities points. For these points, a linear interpolation using ghost cells is performed to obtain the velocitie values according Eq. (12), necessary for discretization of derivatives terms by centered differences.

For example, to calculate the second order derivative term $(u_{xx})_{i+1/2,j}$ in face $(x_{i+1/2}, y_j)$, by centered difference scheme, given by:

$$(u_{xx})_{i+1/2,j} = \frac{u_{i+1/2,j-1} - 2\,u_{i+1/2,j} + u^{g}_{1+1/2,j+1}}{\Delta y^2} \tag{16}$$

The term $u^{g}_{i+1/2,j+1}$ is obtained by an interpolation function presented in Eq. (11), simplified by (Φ), in function of neighbor faces.

$$u^{g}_{i+1/2,j+1} = \Phi\,(u_{\Gamma}, u_{i+1/2,j}, u_{i+1/2,j-1}, u_{i+1/2,j-2}) \tag{17}$$

In order to advance the solution to the time t^{n+1}, is necessary solve the Poisson equation for pressure correction, respecting the condition of incompressible flow, given by discretized equations:

$$\frac{u^{n+1}_{i+1/2,j} - u^{n+1}_{i-1/2,j}}{\Delta x} + \frac{v^{n+1}_{i,j+1/2} - v^{n+1}_{i,j-1/2}}{\Delta x} = 0 \tag{18}$$

$$\frac{p'_{i+1,j}-2\,p'_{i,j}+p'_{i-1,j}}{\Delta x^2}+\frac{p'_{i,j+1}-2\,p'_{i,j}+p'_{i,j-1}}{\Delta x^2}=\frac{u^{n+1}_{i+1/2,j}-u^{n+1}_{i-1/2,j}}{\Delta x}+\frac{v^{n+1}_{i,j+1/2}-v^{n+1}_{i,j-1/2}}{\Delta x} \tag{19}$$

where $p' = p^n - p^{n+1}$. For an arrangement with displaced mesh, is applicate the method of fractional steps (Kim and Moin, 1985), where each step, predictor and corrector, is performed only once.

The Eq. (19) describes the method equation applied in cells away of immersed boundary. Special treatments should be performed in irregular cells. In this case, the pressure equation must have the same treatment of discretization for the velocity. The inactive points will be replaced for ghost values is given by an interpolation or extrapolation function.

The choice of the interpolation function depends on the position of immersed boundary. If the inactive point of velocity it is outside boundary, can be considered a frontier point, and this velocity is treated with an interpolation function, as the Eq. (12). In the case of irregular cells with center nodes lie inside the body, the ghost value is obtained extending the solution beyond of frontier, using a quadratic Lagrange polynomial, as example described by operator (ζ) in Eq. (20) for the velocities and in Eq. (21) for the pressures, in direction *x*.

$$\zeta(u)=\frac{2}{a(a-1)}u^{n+1}_{\Gamma}+\frac{2(a+1)}{a}u_{i-1/2,j}-\frac{a-1}{a+1}u_{i-3/2,j} \tag{20}$$

$$\zeta(p')=\frac{2}{a(a-1)}\frac{\partial p'}{\partial x_{\Gamma}}+\frac{2(a+1)}{a}\left(\frac{p'_{i,j}-p'_{i-1,j}}{\Delta x}\right)-\frac{a-1}{a+1}\left(\frac{p'_{i-1,j}-p'_{i-2,j}}{\Delta x}\right) \tag{21}$$

Where $a\Delta x$ is the distance between the point $x_{i-1/2,j}$ and the immersed boundary. The others variables keep the same as submitted before.

3 RESULTS

3.1 Structural domain

The structural code developed to obtained dynamic behavior of the beam is validated in this section. The modal, harmonic, and transient analyzes were carried out in a cantilever beam. The time responses were obtained by using a Newmark-beta method to solve the associated differential equations. The obtained responses were compared with the ones determined from the software ANSYS® for validation purposes. In the simulations, a cantilever beam with 0.5*x*0.025*x*0.0025 (meters) is used. The Young's modulus, density, and Poisson coefficient are 70 Gpa, 2700 kg/m^3, and 0.33, respectively. The finite element model considered in the simulations and the used conditions are presented in Tab. 1. Table 2 shows the comparison of five first natural frequencies of the beam obtained from the implemented code and the software ANSYS®.

Table 1. Simulation conditions

Data	Values/Comments
Number of elements	30
Excitation nodes (FRF)	31 (free extremity)
Analyzed nodes (FRF)	31,16 (middle)
Proportional damping	$\alpha = 0$; $\beta = 5x10^{-6}$
Frequency band	0 – 500 Hz (steps 1 Hz)
Boundary conditions	Fixed-free

Table 2. Comparison of natural frequencies in [Hz]

Code	ANSYS®	Difference (%)
8,226 Hz	8,225 Hz	0,0122
51,546 Hz	51,545 Hz	0,0019
144,33 Hz	144,32 Hz	0,0069
282,83 Hz	282,79 Hz	0,0141
467,55 Hz	467,45 Hz	0,0214

The frequency response functions (FRFs) were obtained from Eq. (18). Figure 4 show the FRFs obtained from the implemented code and the software ANSYS®.

$$FRF = \frac{1}{[K_{(g)}] + i\omega[C_{(g)}] - \omega^2[M_{(g)}]} \tag{18}$$

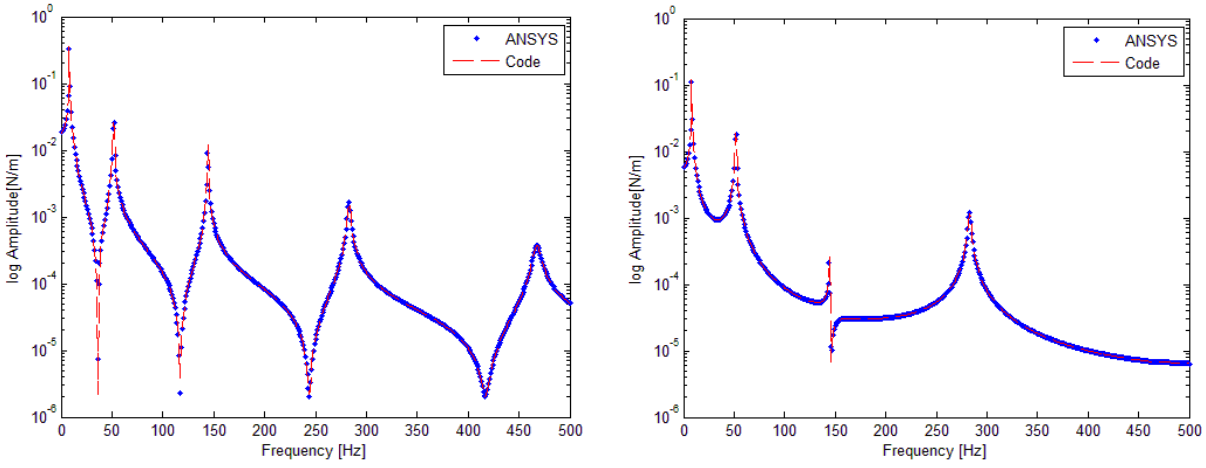

(a) (b)

Figure 4. (a) FRF with entrance in node 31, and analyzed node 31. (b) FRF with entrance in node 31, and analyzed node 16

Figure 5 shows the comparison between the dynamic responses of the cantilever beam obtained from the implemented code and the software ANSYS®. The transient responses of the beam were given by the integration of the equations of motion using a sinusoidal load $F = A\,\sin(2\pi f t)$ applied on the extremity node of beam with 0.5N of amplitude and 5 Hz of frequency (steps of 0.001 seconds).

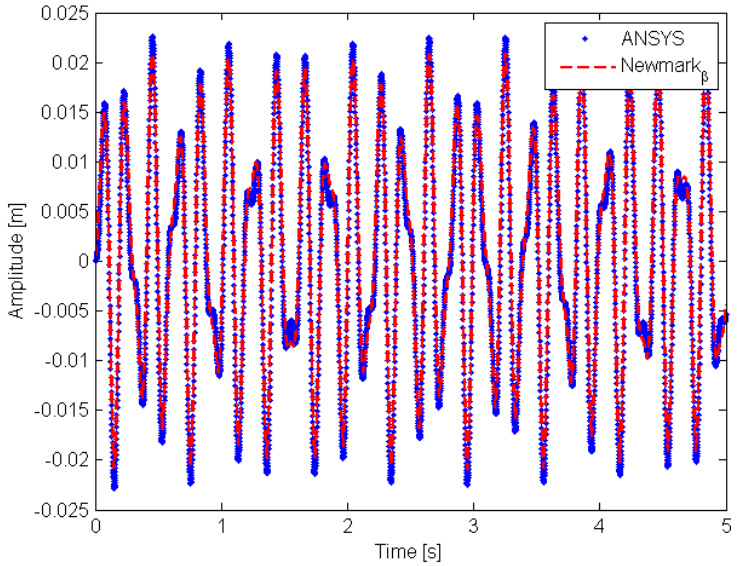

Figure 5. Transient response due to harmonic load.

The results obtained shows the good agreement between the developed code with commercial software of finite elements. The great accordance of results carried out in beam, demonstrate the efficiency of methodology proposed to solve structural domain.

3.2 Fluid domain

Two different geometries are investigated and both are calculated at same Reynolds number (*Re* = 40), they are: flow past a circular cylinder and a two-dimensional normal beam. The circular cylinder results are compared to literature (Countanceau *et al.*, 1977; Russel *et al.*, 2003; Calhoun, 2002; Xu et al., 2006) in order to validate the method. The drag coefficient was defined as $C_D = 2F_D / (\rho U_0{}^2 d)$, where F_D is the drag force, and d is the nominal diameter of cylinder. Dirichlet boundary conditions are used at the inflow $(u / u_\infty = 1; v = 0)$ and at the cylinder surface $(u = 0; v = 0)$. A Neumann-type boundary conditions is adopted at the outflow and farfield boundaries.

Flow past a 2D stationary circular cylinder

Laminar flows past a two-dimensional circular cylinder is a classic benchmark problem. The results are compared to literature to verify the method presented in this work. For the simulations at *Re* = 40, a non-uniform grid of 28,000 cells is used. Figure 6 shows the sketch of a computational domain and the grid used on simulations.

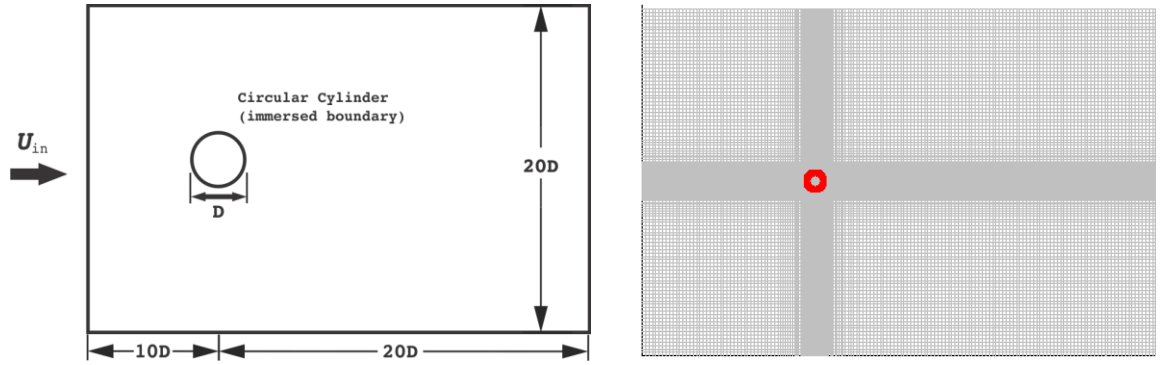

(a) (b)

Figure 6. (a) Schematics of the domain flow around a circular cylinder. (b) Computational non-uniform cartesian mesh was used on simulation.

The comparison of the drag coefficient obtained in the present work with other numerical and experimental results are presented in Tab. 4. The nomenclature is presented in Fig. 7. It can be observed that good agreement was obtained.

Table 3. Comparison of characteristics in flow past a cylinder (*Re* = 40)

	L/D	*a/D*	*b/D*	θ	C_D
Coutanceau e Bouard (1977)	2,13	0,76	0,59	53,5	1,53
Calhoun (2002)	2,18	-	-	54,2	1,52
Russel e Wang (2003)	2,29	-	-	53,1	1,51
Xu e Wang (2006)	2,21	-	-	53,5	1,54
Present Study	***2,28***	***0,77***	***0,60***	***55,0***	***1,546***

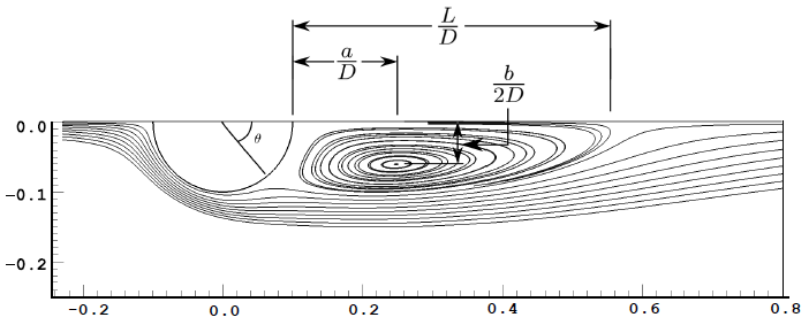

Figure 7. Characteristics in flow past a circular cylinder at *Re*=40 (ANDRADE, 2015)

Figure 8 shows, respectively, the streamlines, iso-vorticity contours and the iso-pressure contours for a stationary circular cylinder.

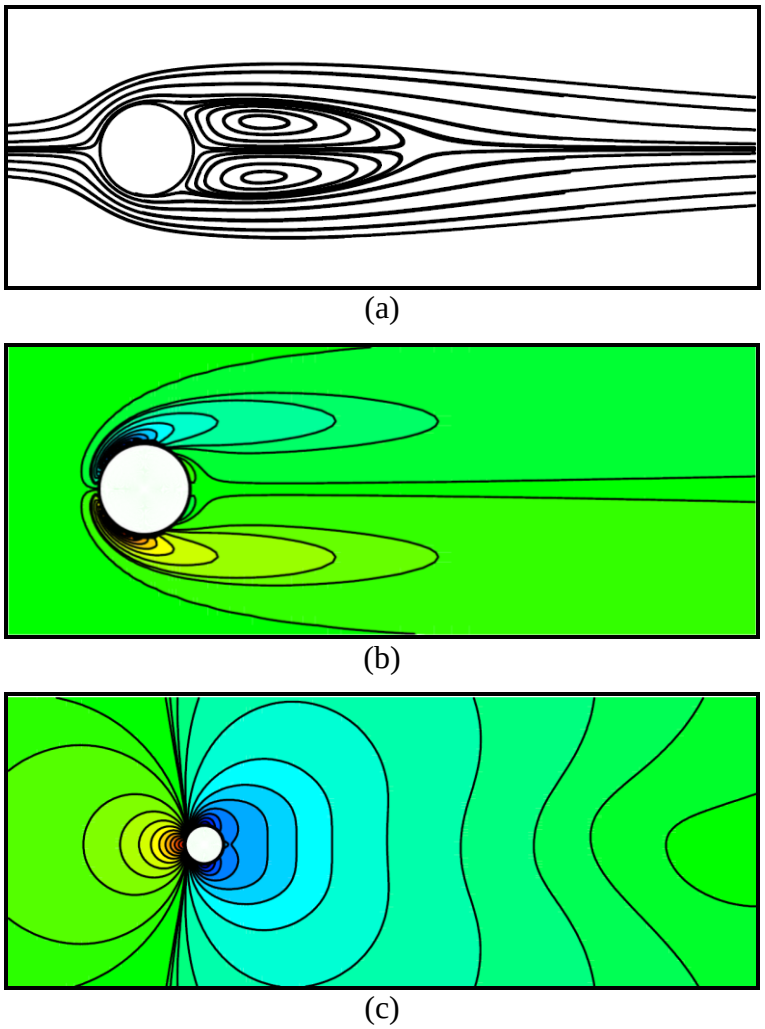

Figure 8. Flow past a cylinder: (a) streamlines, (b) iso-vorticity contours and (c) iso-pressure contours at *Re*=40.

The results show the good accordance with studied literature and demonstrate the efficient of proposed method to simulate flows even on blunt bodies as a cylinder.

Flow past a 2D normal beam

Finally, the problem of a cantilever beam proposed for study of fluid-structure problem is investigated. The sharp structure presented in section 3.1 is tested by the LGC method in a flow channel. For the simulations at *Re* = 40, a uniform grid of 40,000 cells is used. Figure 9 shows the sketch of a computational domain used on simulations.

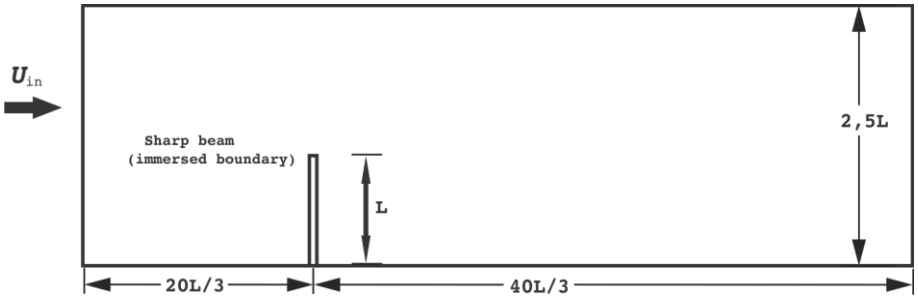

Figure 9. Schematics of the confined flow around a sharp beam

The simulation was performed such that the thickness of geometry is smaller than one cell grid. Thus, the method of local ghost cells to solve incompressible flows over thin bodies is fully tested.

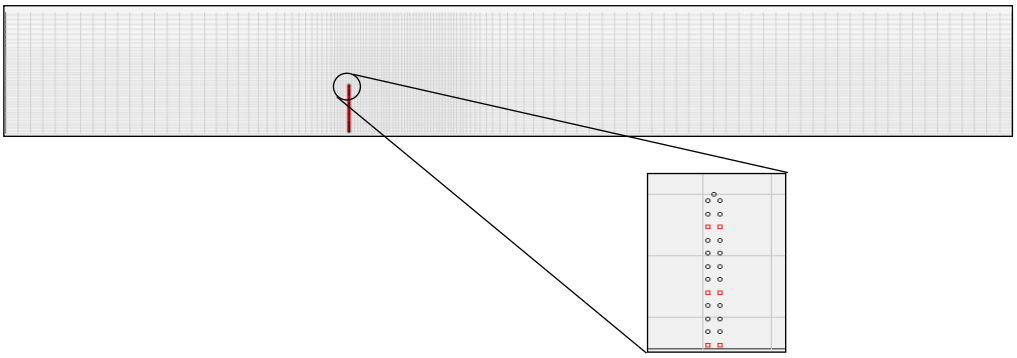

Figure 10. Detail of discrete points of beam inside a fluid cell

Figure 11 presents, respectively, the velocity and pressure fields, and iso-vorticity contours for the simulation over the beam. It can be observed that the dynamic pressure is higher upstream the beam, which would lead to a displacement of the geometry when considered a structural coupling.

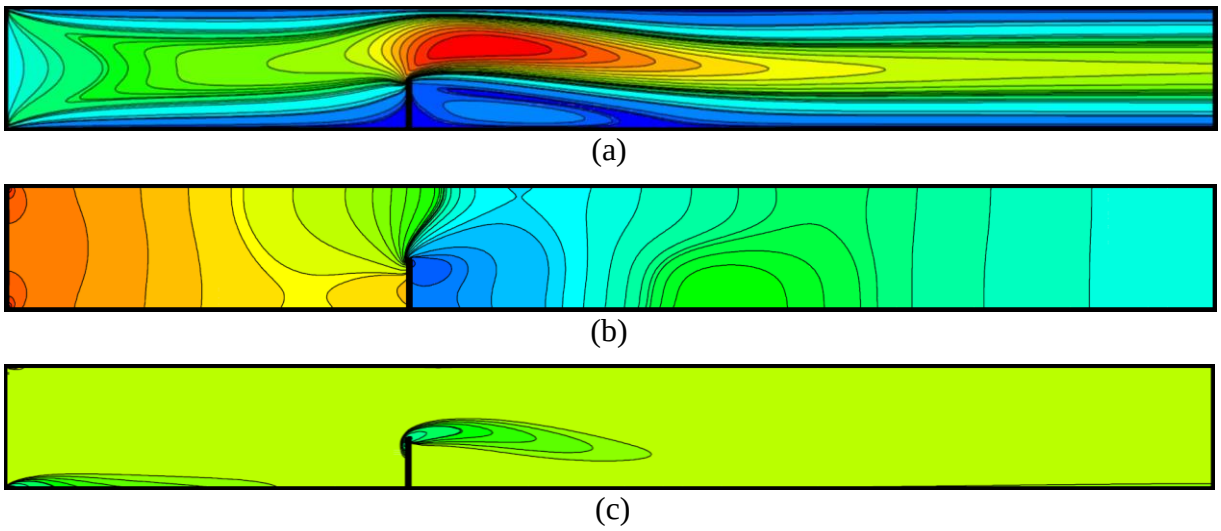

(a)

(b)

(c)

Figure 11. Confined flow over a beam: (a) velocity field; (b) pressure field; (c) iso-vorticity contour

Details of the simulated flow are presented in Fig. 11. It can be noticed that for the parameters employed, there is almost no noticeable difference between the vortices downstream the cylinder. For the highly irregular geometry presented, the local feature of the present method allows be treated accurately. Further efforts will be dedicated to implement moving bodies in the fluid code for coupling with the structural code presented earlier.

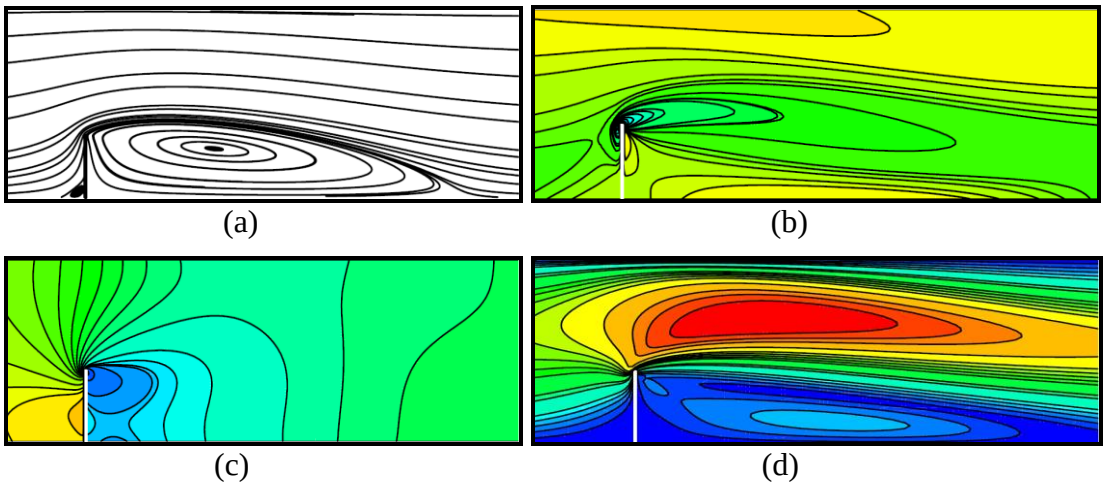

Figure 11. Details of confined flow over a beam. (a) Streamlines at *Re*=40; (b) Iso-vorticity contours; (c) Pressure field; (d) Velocity field

4 FINAL REMARKS

Immersed boundary methods (IBM) have emerged as a powerful numerical approach for simulating fluid structure problems in engineering. The hallmark of these methods is their inherent ability to handle complex deformable bodies without the need to construct grids that conform and deform with solid boundaries. A limitation of immersed boundary methods is their inability in deal with corners and sharp geometries, as beams and airfoils.

The present work investigates a branch of IBM and your efficiency in solve the problem proposed in this work. Both the structural and fluid codes developed show good results to problem presented. Future work should focus on a coupling algorithm, take into account the implement of moving boundaries and transfer loads to the finite element code.

ACKNOWLEDGEMENTS

The authors are thankful to CNPQ, PROPP, CAPES, PETROBRAS and FAPEMIG for the financial support and the School of Mechanical Engineering of the Federal University of Uberlândia for the technical support provided to this research.

REFERENCES

Andrade, J.R., 2015. *Immersed Boundary Methods for sharp-shaped geometries: implementation and validation (In Portuguese)*. Master's thesis, Programa de Pós Graduação em Engenharia Mecânica da Universidade Federal de Uberlandia.

Berthelsen, P.A. and Faltinsen, O.M., 2008. "A local directional ghost cell approach for incompressible viscous flow problems with irregular boundaries." Journal of Computational Physics, Vol. 227, 4354-4397.

Calhoun, D. A cartesian grid method for solving the two-dimensional streamfunction-vorticity equations in irregular regions. *J. Comput. Phys.*, v. 176 :231-275, 2002. 88, 90

Countanceau, M.; Bouard, R. "Experimental determination of the main features of the viscous flow in the wake of a circular cylinder in uniform translation part 1". *Steady flow. J. Fluid Mech.*, v. 79:231-256, 1977. 88, 90

Farhat C.; Lesoinne, M.; Letallec, P. Load and motion transfer algorithms for fluid/structure interaction problems with non-matching discrete interface: Momentum and Energy conservation, optimal discretization and application to aeroelasticity. *Comput. Methods Appl. Mech. Engrg***.** n.157, p. 95-114. 1998.

Hutton, D.V. *Fundamentals of finite element analysis*. 2004, McGraw Hill, 505s

Mitra, S.; Sinhamahapatra, K.P. 2D simulation of fluid-structure interaction using finite element method. J. Finite Elements in Analysis and Design 45 (2008) 52 -59

Russel, D.; Wang, Z. A cartesian grid method for modeling multiple moving objects in 2d incompressible viscous flow. *J. Comput. Phys.*, v. 191:177-205., 2003. 90

Xu, S.; Wang, Z. An immersed interface method for simulating the interaction of a fluid with moving boundaries. *J. Comput. Phys.*, v. 216:454-493., 2006. 90